RSC Advances

ROYAL SOCIETY OF CHEMISTRY

www.rsc.org/advances

Carbon-protected Au Nanoparticles Supported on Mesoporous TiO_2 for Catalytic Reduction of *p*-nitrophenol

Tuo Ji, Licheng Li, Meng Wang, Zhuhong Yang*, and Xiaohua Lu

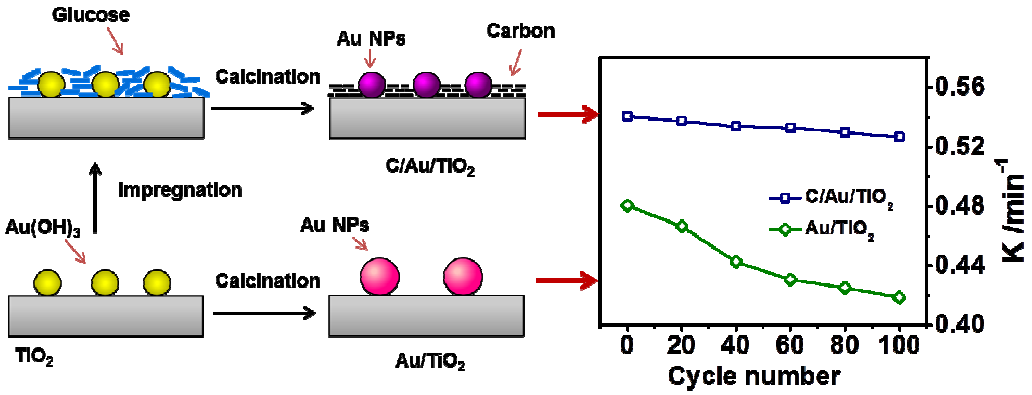

With introduction of carbon on Au/TiO_2, the reaction rate of $C/Au/TiO_2$ increased by 29% and stability enhanced about 3 times than Au/TiO_2 in the *p*-nitrophenol reduction reaction. Carbon species enhanced the stability of Au nanoparticles and also increase the organic reactants adsorptive ability

Cite this: DOI: 10.1039/c0xx00000x

www.rsc.org/xxxxxx

ARTICLE TYPE

Carbon-protected Au Nanoparticles Supported on Mesoporous TiO_2 for Catalytic Reduction of *p*-nitrophenol

Tuo Ji[1], Licheng Li[2], Meng Wang[1], Zhuhong Yang*[1], and Xiaohua Lu[1]

Received (in XXX, XXX) Xth XXXXXXXXX 20XX, Accepted Xth XXXXXXXXX 20XX

DOI: 10.1039/b000000x

With introduction of carbon on Au/TiO_2, the reaction rate of C/Au/TiO_2 increased by 29% and stability enhanced about 3 times than Au/TiO_2 in the *p*-nitrophenol reduction reaction. Carbon species enhanced the stability of Au nanoparticles and also increase the organic reactants adsorptive ability

Supported gold catalysts have drawn tremendous attention due to their high catalytic activity and efficiency for a broad range of chemical reactions including CO oxidation[1,2], selective hydrogenation[3,4], methanol synthesis[5,6] and water-gas shift[7-9]. Numerous studies have found that the activity of gold catalysts was largely dependent on its particle size and dispersion[10]. However, with the decrease of the size of Au NPs, the nanosized Au NPs easily move and grow on most of the metal oxide surfaces. Once NPs aggregation occurs and the particle size increases to micro-metric scale, the activity of Au NPs could disappear completely. Thus, Au NPs aggregation is still an obstacle to the industrial application particularly in reaction systems[11]. In order to ameliorate the stability of Au NPs on the support surface, researchers focus on incorporating additional components(SiO_2, TiO_2, FeO_X et al) which attempt to anchor Au NPs and prevent aggregation[12-15]. Compared with these metal oxides, carbon is affordable, easily prepared, and chemical inertness, which would not bring unexpected side reactions in industrial reaction processes. Another important role of carbon is the adsorption ability of organics in the solution which could promote mass transfer in catalyst-related process[16]. Here, we report an *in-situ* carbonization method to improve the *p*-nitrophenol reduction rate and stability of Au/TiO_2 catalyst.

In our previous work, mesoporous TiO_2 was prepared from potassium titanate via hydration and ion-exchange[17]. The corresponding gold catalyst exhibited excellent catalytic performance as well as good stability due to mesoporous structure[18,19]. In order to improve catalyst performance and stability, we introduced a layer of carbon on the surface of gold catalyst. As Fig. 1a shows, the Au/TiO_2 was coated with a layer of glucose, followed by in situ carbonization of the glucose at 500ºC to leave a base of carbon at the catalyst surface. Compare with the Au/TiO_2 calcincated at the same temperature, the aggregation of Au NPs was limited and the size of Au NPs in C/Au/TiO_2 smaller than that in Au/TiO_2. The detailed carbon modification processes are described in ESI. †

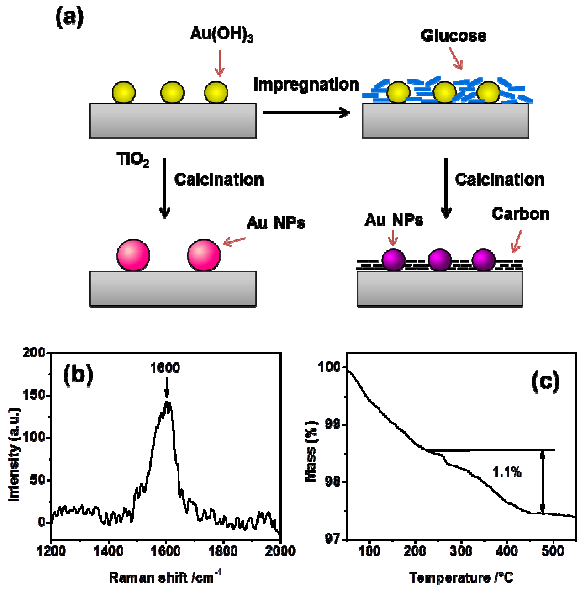

Fig. 1(a) Schematic illustration of the C/Au/TiO_2 and Au/TiO_2 preparation. (b) Raman spectrum and (c) TG curve of C/Au/TiO_2.

Raman analysis of C/Au/TiO_2 was used to identify the carbon species on TiO_2 (Fig. 1(b)). It shows a characteristic G-band at around 1600 cm^{-1} and a weak D-band at around 1340 cm^{-1}, indicating that the carbon species is graphitized carbon[20,21]. Carbon content in the C/Au/TiO_2 catalysts was measured by TG. As illustrated in Fig. 1(c), the sample weight loss before 300 °C was ascribed to the removal of physically adsorbed water and impurity. The weight loss from 300 °C to 500 °C is mainly due to the burn out of carbon species[22]. The carbon content could be less than 1.1 wt%.

XRD analyses show the crystalline structures of TiO_2, Au/TiO_2, and C/Au/TiO_2 (Fig. S1 in ESI †). Seven distinct

[1]*State Key Laboratory of Material-Oriented Chemical Engineering, College of Chemistry and Chemical Engineering, Nanjing Tech University, Nanjing 210009, P. R. China.*

[2] *College of Chemical Engineering, Nanjing Forestry University, Nanjing 210037, Jiangsu, China*

E-mail: zhhyang@njut.edu.cn; Tel: +86-25-83172251

† Electronic supplementary information (ESI) available: Experimental details and additional characterization data. See DOI: 10.1039/b000000x/

diffraction peaks of three samples are indexed to anatase (JCPDF 21-1272) with high crystallinity, while weak peaks corresponding to the TiO_2 (B) phase (JCPDF 35-0088) can be observed. These results are consistent with previously report[18]. The average TiO_2 crystal size was about 11 nm, as reckoned from the peak width of the anatase (101) peak by using the Scherrer equation. Such common characteristics of these three samples show that they have the same crystal structure. It reveals that the carbon species may not influence the catalysts structure and dispersion of active species. However, the presence of diffraction peaks of Au was dim probably owing to its low content and small particle size. The Barrett-Joyner-Halenda (BJH) pore-size analyses from the N_2 desorption curve reveals that three samples exhibit almost identical pore-size distributions ranging from 6 to 12 nm with a mean pore size around 9 nm (Fig. S2 in ESI †). Table 1 summarized the specific surface area of each sample, 112.5 m^2g^{-1} for TiO_2, 112.1 m^2g^{-1} for Au/TiO_2, and 108.5 m^2g^{-1} for $C/Au/TiO_2$, which was calculated by the multi-point Brunauer-Emmett-Teller (BET) method. These observations demonstrate that catalyst structure was maintained even after introducing carbon materials.

Table 1 Physical structure properties and catalytic performance of samples

Sample	Crystal Size /nm	S_{BET} /$m^2 \cdot g^{-1}$	V_P /$cm^3 \cdot g^{-1}$	Au loading$^{\alpha}$ /wt%	$d_{Au}{}^{\beta}$ /nm	k /min^{-1}
TiO_2	11.2	112.5	0.19	-	-	-
Au/TiO_2	11.2	112.1	0.19	0.871	5.5 ±1.5	0.44
$C/Au/TiO_2$	11.3	108.5	0.16	0.861	4.1 ±1.0	0.57

$^{\alpha}$: The content of Au was analyzed by XRF.

$^{\beta}$: The size of Au NPs was evaluated by FESEM statistics

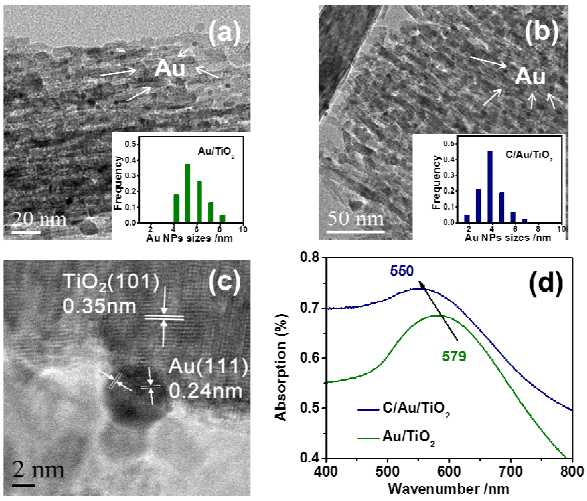

Fig. 2 (a) TEM images of Au/TiO_2. Inset: size distribution of Au NPs; (b) TEM images of $C/Au/TiO_2$. Inset: size distribution of Au NPs; (c) HRTEM images of $C/Au/TiO_2$; (d) UV-vis spectra of $C/Au/TiO_2$ and Au/TiO_2.

The morphology of Au NPs was further studied by TEM. As shown in the Fig. 2(a, b), Au NPs dispersed on mesoporous TiO_2 were observed. The lattice fringe of 0.35 nm corresponds to the (101) plane of anatase[23]. A representative high-resolution TEM (HRTEM) image (Fig. 2(c)) shows that Au NPs are highly crystalline as evidenced from the well resolved Au lattice fringes of 0.24 nm ((111) plane of Au)[23]. With the incorporation of carbon, Au NPs size in $C/Au/TiO_2$ became smaller than that of Au/TiO_2 catalyst, and an uniform particle size distribution at 4 nm is observed in the inset of Fig. 2(a, b).

The Au NPs dispersion was also performed by UV-vis absorption spectroscopy. Fig. 2(d) shows that $C/Au/TiO_2$ and Au/TiO_2 both have an absorption peak in the visible region (from 550 to 580 nm). This peak can be attributed to the surface plasma absorption (SPA) of the Au NPs[24]. For $C/Au/TiO_2$, the absorption peak is at around 550 nm, which is lower than that of Au/TiO_2 (around 579 nm). The entire absorption peak in the visible region of Au/TiO_2 displays a larger red shift compared with that of $C/Au/TiO_2$. This red-shift was attributed to the gather of Au NPs as reported in the literature.[23] Au NPs on the surface of TiO_2 agglomerated after 500 °C, which cause the decreased distance among them. Apparently, this red shift demonstrates that Au NPs of $C/Au/TiO_2$ have a better dispersions and smaller sizes, which were also previously confirmed by TEM statistics analysis.

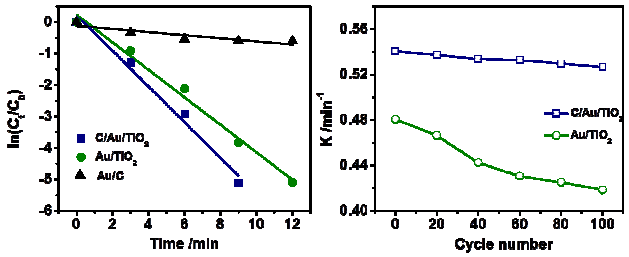

Fig. 3(a) Plot of $\ln(C_t/C_0)$ versus reaction time of aqueous phase reduction of PNP by $NaBH_4$ over different gold catalysts. (b) Reuse cycles of newly catalysts for PNP reduction

Reduction of *p*-nitrophenol by an excess amount of $NaBH_4$ is chosen as a model reaction to evaluate the catalytic performances of the Au catalysts. It is well-known that the reaction is simple and steady in the presence of metallic surfaces. The Au NPs played a key role as an electron transfer mediator between BH_4^- and PNP molecules. The maximum UV-Vis absorption peak of the aqueous mixture of PNP and $NaBH_4$ stayed unaltered at 400 nm with time. Reaction mixture causes fading as the catalyst added. The reaction kinetics could be analyzed and confirmed from the time-dependent absorption spectra, which showed the gradually decrease of *p*-nitrophenolate ions[25,26]. Fig. 3(a) shows linear relation of $\ln(C_t/C_0)$ versus reaction time by using $C/Au/TiO_2$, Au/TiO_2 and Au/C. The ratio of C_t and C_0, where C_t and C_0 represent PNP concentrations at time t and 0, respectively, was measured from the relative intensity of the respective absorbencies. The linear relations of $\ln(C_t/C_0)$ versus time were observed for all the tested catalysts, indicating that the PNP reduction reaction followed the pseudo-first-order kinetics. In this study, $C/Au/TiO_2$ exhibited a better PNP reduction performance than that of Au/TiO_2. The reaction rate constant is 0.44 min^{-1} calculated from the slope of Au/TiO_2, which is comparable to other gold catalysts reported recently[27-30]. However, with the introduction of carbon, the reaction rate constant of the $C/Au/TiO_2$ increased to 0.57 min^{-1}, which is 29% higher than Au/TiO_2. Surface carbon species on gold catalyst is

beneficial to the improvement in the PNP reduction by $NaBH_4$, which is partly related to the smaller size and better dispersion of Au NPs

Besides, Au/C shows relatively low reaction rate. The reaction rate constant is only 0.06 min^{-1} and almost reaches to zero after 6 min. It suggests that interaction between C and Au is not the important reason of the performance enhancement. But carbon on the surface of the catalyst might accelerate efficiency of mass transfer (Fig. S3 in ESI†). Obviously, the PNP absorption on $C/Au/TiO_2$ is about 37% after 1 min, while it is only 11% on Au/TiO_2. Although both of absorption amount are about the same when reach absorptive equilibrium, PNP adsorptive velocity of catalysts is increased by carbon. The carbon might change the hydrophilic performance of catalyst surface, which make nitrophenol easily transfer from aqueous phase to catalyst surface. Hence, carbon species on the surface of gold catalysts enhanced the activity, which could be attributed to two factors: (1)the Au NPs of $C/Au/TiO_2$ have the smaller size and the better dispersion and (2) the increase of p-nitrophenol adsorptive ability by carbon.

For industrial applications of view, reusability and recovery performance is the main concern of a heterogeneous catalyst. Fig. 3(b) shows that reuse cycles of novel catalysts were evaluated for PNP reduction. The catalyst particles were immediately separated from the reaction mixture by simple centrifugation at 6000 RPM. Then experiments were performed by keeping all other factors constant. The results revealed that $C/Au/TiO_2$ shows good activity after 100 reaction cycles. The reaction rate constant of the $C/Au/TiO_2$ is 0.52 min^{-1}, which only dropped by 4%. However, the reaction rate constant of Au/TiO_2 dropped 12.5% from 0.48 min^{-1} to 0.42 min^{-1}. It can be seen that the stability of $C/Au/TiO_2$ catalysts enhanced about 3 times than Au/TiO_2 catalysts. Therefore, carbon species further enhance the stability of catalyst and prevent the deactivation of the catalyst.

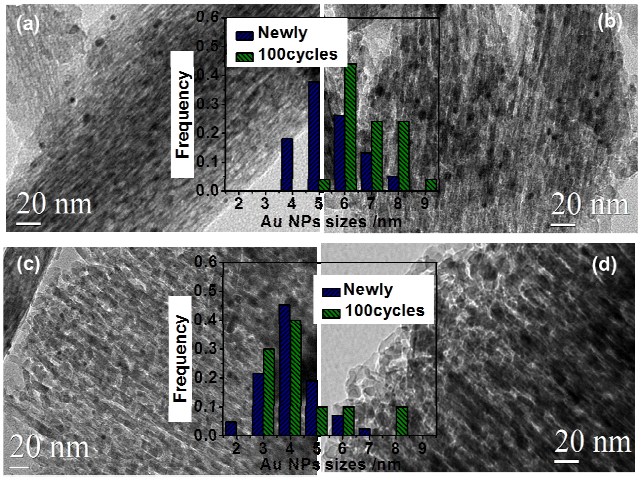

Fig. 4 TEM images of Au/TiO_2 before (a) and after 100 cycles reaction (b), $C/Au/TiO_2$ before (c) and after 100 cycles reaction (d), the insets are the size distribution of Au NPs corresponding to each change of catalysts.

Fig. 4 shows the change in sizes of Au NPs for the catalysts before and after 100 cycles PNP reduction reaction. The size distributions of Au particles are summarized from six images of each sample, shown in the insets of Fig. 8. After reaction, Au NPs on Au/TiO_2 agglomerated and become larger as demonstrated by a size distribution from 5.5 ± 1.5 nm to 7.05 ± 1.0 nm, while the size distribution of Au NPs on $C/Au/TiO_2$ showed good stability with a minor change from 4.1 ± 1.0 nm to 4.5 ± 2.0 nm. Therefore, carbon species help to enhance the stability of Au NPs on the TiO_2 surface.

In summary, we prepared a carbon surface modification of Au nanoparticles supported on TiO_2 catalysts. Carbon species has no influence on the structure of catalyst but can enhance stability and activity of Au catalysts in the hydrogenation of *p*-nitrophenol reaction. With less than 1.1% carbon protected, the activity of $C/Au/TiO_2$ was enhanced 29% by carbon introduction. In addition, we also found the presence of carbon promotes the adsorption of reactant during reaction. After 100-cycle PNP reduction reaction, $C/Au/TiO_2$ presented more stable activity than Au/TiO_2. The carbon modification on nanocrystal supports can be a viable route to tailor the stability and activity of supported catalysis system. The detailed structural mechanism for the enhanced stability is currently under investigation.

This work was financially supported by the Major Program of National Natural Science Foundation of China (91334202), Chinese National Key Technology Research and Development Program (Grant No. 2006AA03Z455) and the National Natural Science Foundation of China (Grant Nos. 21136001, 21136004, 20976080, 21206070)

References

1 Camellone, M. F.; Fabris, S. *Journal Of the American Chemical Society* 2009, **131**, 10473.
2 Green, I. X.; Tang, W. J.; Neurock, M.; Yates, J. T. *Science* 2011, **333**, 736.
3 Bus, E.; Prins, R.; van Bokhoven, J. A. *Catalysis Communications* 2007, **8**, 1397.
4 Hugon, A.; Delannoy, L.; Louis, C. *Gold Bulletin* 2008, **41**, 127.
5 Sakurai, H.; Haruta, M. *Catalysis Today* 1996, **29**, 361.
6 Sakurai, H.; Tsubota, S.; Haruta, M. *Applied Catalysis a-General* 1993, **102**, 125.
7 Burch, R. *Physical Chemistry Chemical Physics* 2006, **8**, 5483.
8 Idakiev, V.; Tabakova, T.; Tenchev, K.; Yuan, Z.-Y.; Ren, T.-Z.; Su, B.-L. *Catalysis Today* 2007, **128**, 223.
9 Hinojosa-Reyes, M.; Rodríguez-González, V.; Zanella, R. *RSC Advances* 2014, **4**, 4308.
10 Haruta, M.; Tsubota, S.; Kobayashi, T.; Kageyama, H.; Genet, M. J.; Delmon, B. *Journal of Catalysis* 1993, **144**, 175.
11 Sandoval, A.; Louis, C.; Zanella, R. *Applied Catalysis B: Environmental* 2013, **140**, 363.
12 Ma, Z.; Dai, S. *Nano Research* 2011, **4**, 3.
13 Ma, Z.; Brown, S.; Howe, J. Y.; Overbury, S. H.; Dai, S. *J. Phys. Chem. C* 2008, **112**, 9448.
14 Guczi, L.; Frey, K.; Beck, A.; Peto, B.; Daroczi, C. S.; Kruse, N.; Chenakin, S. *Applied Catalysis a-General* 2005, **291**, 116.
15 Rodríguez-González, V.; Zanella, R.; Calzada, L. A.; Gómez, R. *The Journal of Physical Chemistry C* 2009, **113**, 8911.
16 Bandosz, T. J.; Petit, C. *Journal of Colloid and Interface Science* 2009, **338**, 329.

17 He, M.; Lu, X. H.; Feng, X.; Yu, L.; Yang, Z. H. *Chem. Commun.* 2004, 2202.
18 Zhu, Y.; Li, W.; Zhou, Y.; Lu, X.; Feng, X.; Yang, Z. *Catalysis Letters* 2009, **127**, 406.
19 Li, L.; Wang, C.; Ma, X.; Yang, Z.; Lu, X. *Chinese Journal of Catalysis* 2012, **33**, 1778.
20 Ferrari, A. C.; Robertson, J. *Physical Review B* 2000, **61**, 14095.
21 Eklund, P. C.; Holden, J. M.; Jishi, R. A. *Carbon* 1995, **33**, 959.
22 Li, L.; Zhu, Y.; Lu, X.; Wei, M.; Zhuang, W.; Yang, Z.; Feng, X. *Chem. Commun.* 2012, **48**, 11525.
23 Li, H.; Bian, Z.; Zhu, J.; Huo, Y.; Li, H.; Lu, Y. *Journal of the American Chemical Society* 2007, **129**, 4538.
24 Boccuzzi, F.; Cerrato, G.; Pinna, F.; Strukul, G. *Journal of Physical Chemistry B* 1998, **102**, 5733.
25 Dotzauer, D. M.; Dai, J.; Sun, L.; Bruening, M. L. *Nano Letters* 2006, **6**, 2268.
26 Kuroda, K.; Ishida, T.; Haruta, M. *Journal of Molecular Catalysis a-Chemical* 2009, **298**, 7.
27 Ismail, A. A.; Hakki, A.; Bahnemann, D. W. *Journal of Molecular Catalysis a-Chemical* 2012, **358**, 145.
28 Han, L.; Zhu, C. Z.; Hu, P.; Dong, S. J. *Rsc Advances* 2013, **3**, 12568.
29 Kong, L. C.; Duan, G. T.; Zuo, G. M.; Cai, W. P.; Cheng, Z. X. *Materials Chemistry and Physics* 2010, **123**, 421.
30 Tamiolakis, I.; Fountoulaki, S.; Vordos, N.; Lykakis, I. N.; Armatas, G. S. *Journal of Materials Chemistry A* 2013, **1**, 14311.

